

Supplementary Information

Tailorable multifunctionalities in ultrathin 2D Bi-based layered supercell structures

Zihao He^a, Xingyao Gao^b, Di Zhang^b, Ping Lu^c, Xuejing Wang^b, Matias Kalaswad^a, Bethany Rutherford^b, Haiyan Wang^{a,b,*}

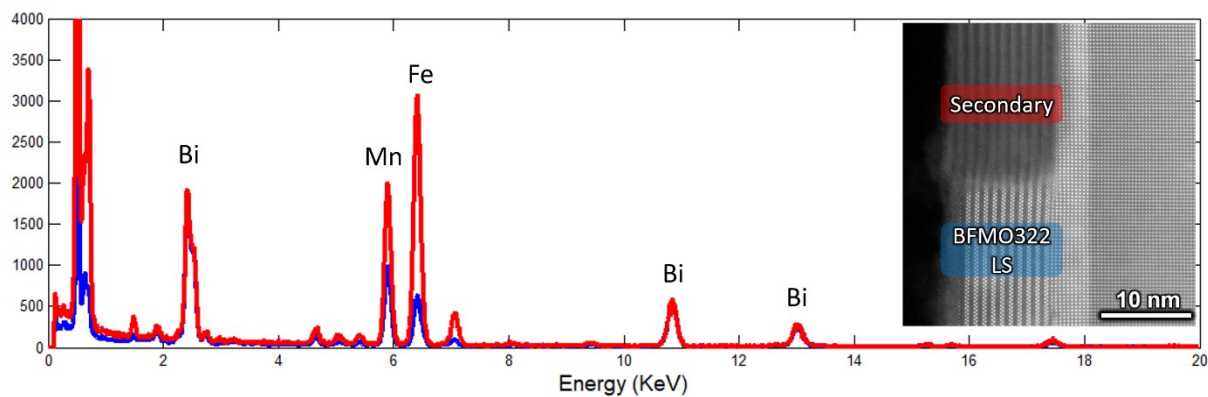


Figure S1. EDS spectra for the secondary phase (red line) and BFMO 322 LS (blue line), the inset presents the corresponding STEM image.

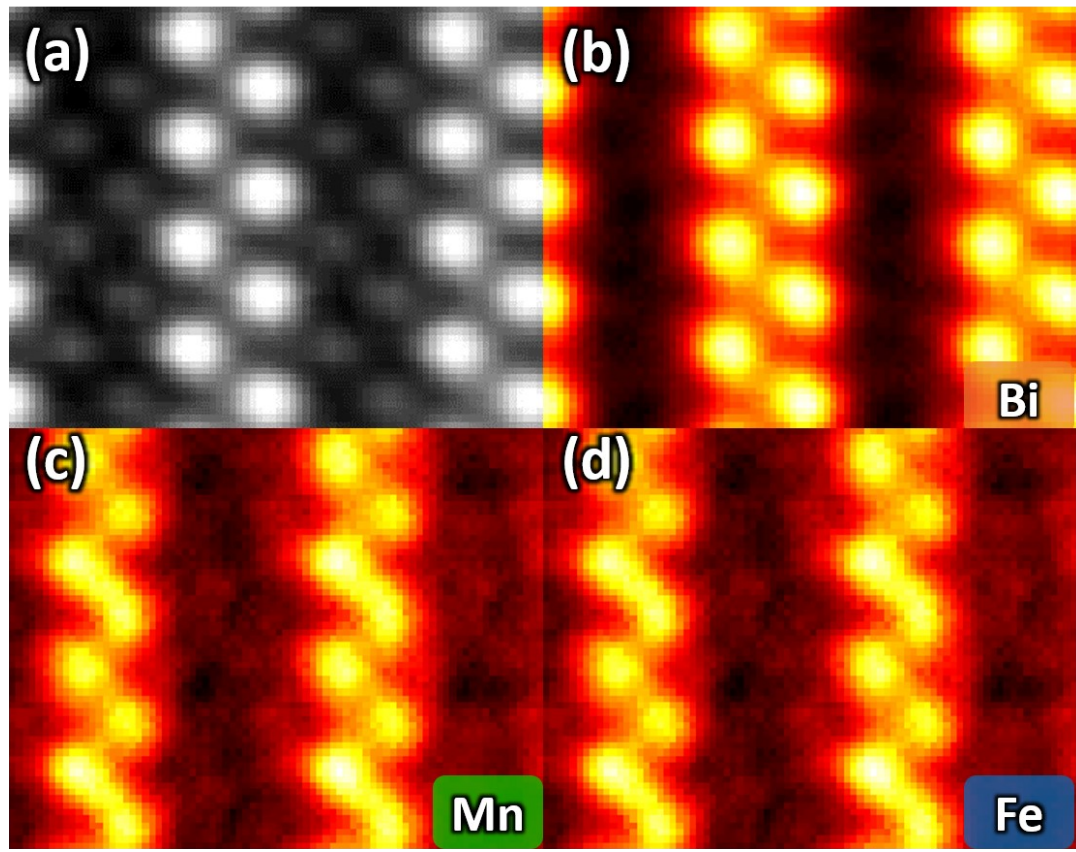


Figure S2. (a) HR-STEM image of BFMO322 LS structure. (b-d) Atomic resolution color EDS maps of Bi, Mn, and Fe atoms in the BFMO322 LS structure, identifying Bi_2O_2 slabs and distorted $\text{FeO}_6/\text{MnO}_6$ octahedra.

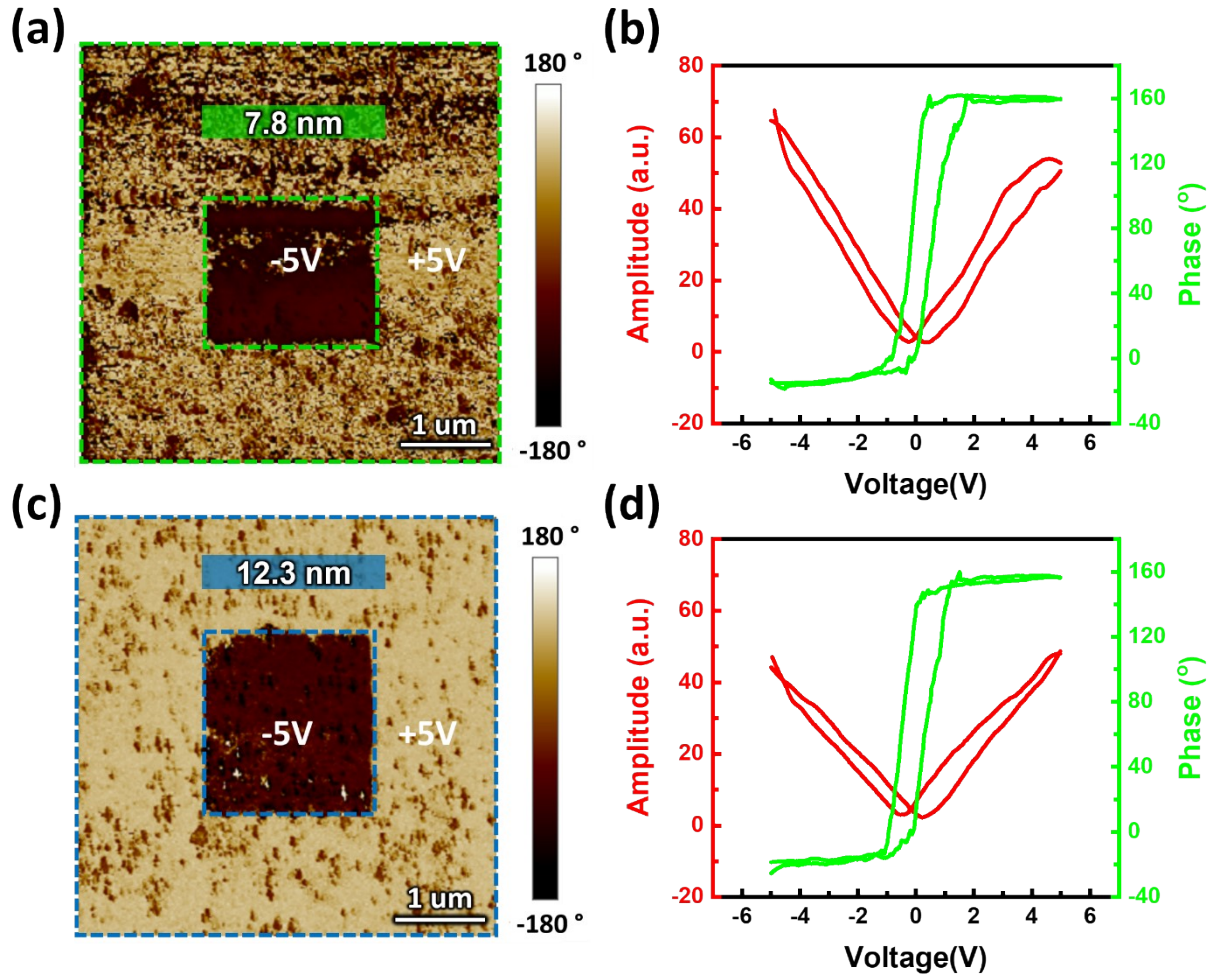


Figure S3. PFM vertical phase map of (a) 7.8 nm, and (c) 12.3 nm BFMO films after +5V writing over a $5 \times 5 \mu\text{m}^2$ square box followed by -5V rewriting over a $2 \times 2 \mu\text{m}^2$ central square box. The amplitude (red) and phase (green) switching curves of (b) 7.8 nm, and (d) 12.3 nm BFMO films as a function of bias voltage.

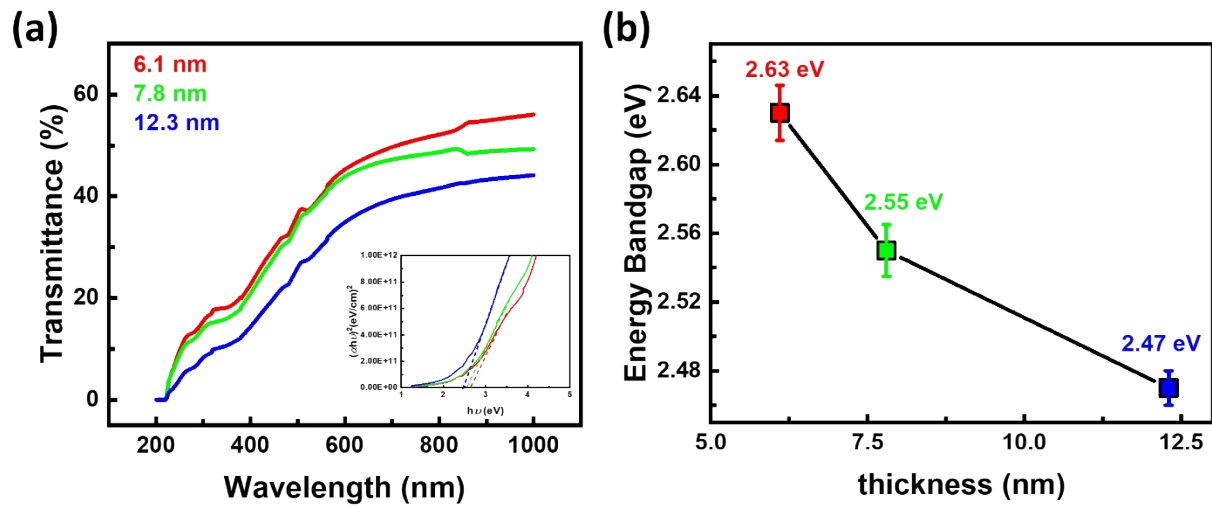


Figure S4. (a) The optical transmittance spectra of BFMO films with three different thicknesses as a function of wavelength. The inset shows the corresponding Tauc-plots. (b) direct band gaps of BFMO films as a function of film thickness.

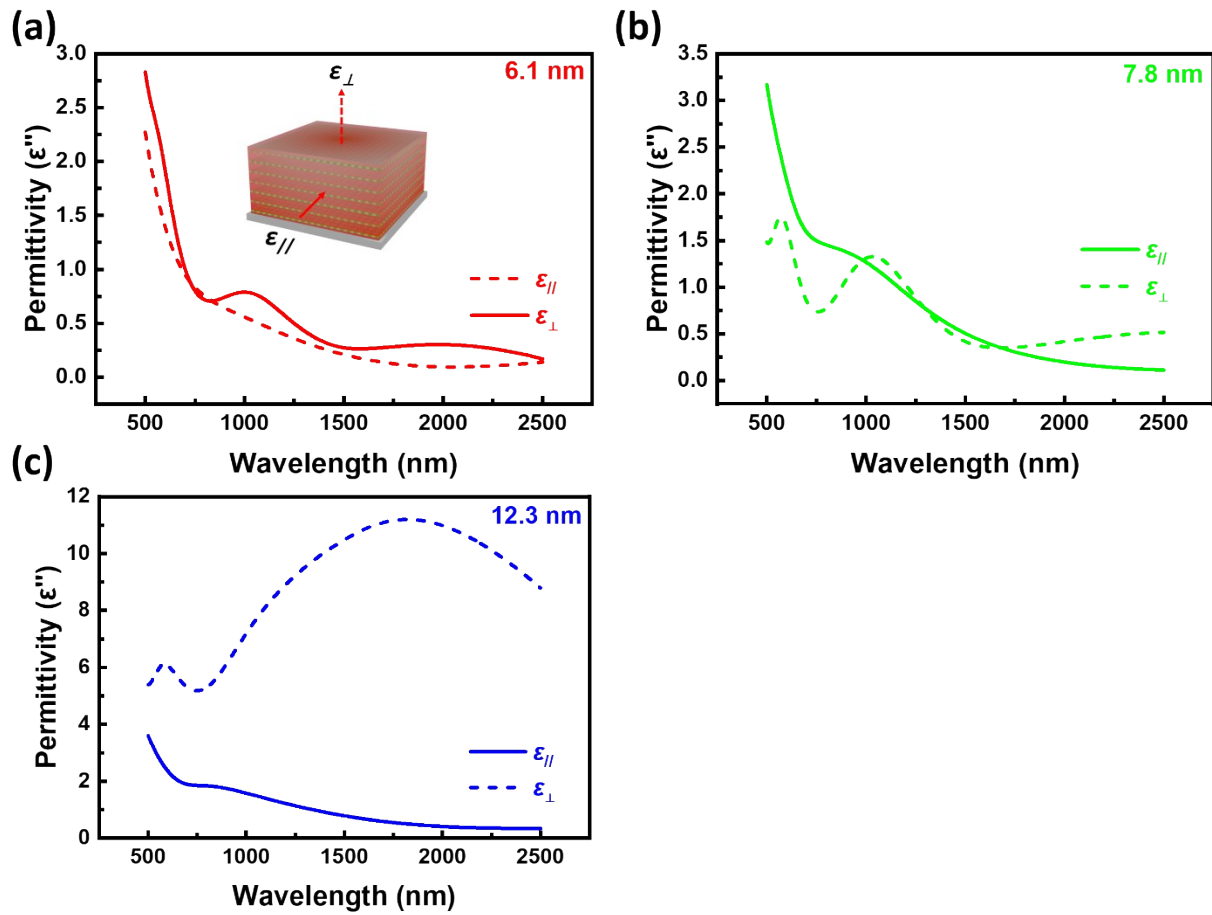


Figure S5. Imaginary part of the permittivity of (a) 6.1 nm, (b) 7.8 nm, and (c) 12.3 nm BFMO films in both IP (solid line) and OP (dashed line) directions.